

Site-dependent lattice dynamics of photoinduced structural change

Kunio Ishida*

Corporate Research and Development Center, Toshiba Corporation, 1 Komukaitoshiba-cho, Saiwai-ku, Kawasaki 212-8582, Japan

Keiichiro Nasu

Solid State Theory Division, Institute of Materials Structure Science, KEK, CREST JST, Graduate University for Advanced Study, 1-1 Oho, Tsukuba, Ibaraki 305-0801, Japan

(Received 19 May 2009; published 1 October 2009)

We study the lattice dynamics of photoinduced structural change by a model of localized electrons coupled with an optical phonon mode. We found that the deformation of individual molecular units obey the large deviation statistics, and found that we can discuss the dynamics before/after structural change separately. We also found that the characteristic vibrational frequencies differ between the molecular units, which reflects the details of the dynamics of the nucleation processes. Thus, by studying the distribution of the relevant phonon frequencies by transient vibrational spectroscopy, the dynamical properties of photoinduced structural change will be experimentally revealed.

DOI: [10.1103/PhysRevB.80.140301](https://doi.org/10.1103/PhysRevB.80.140301)

PACS number(s): 63.20.kd, 71.10.Li, 05.45.-a, 64.60.qe

Recent progress on the study of photoinduced cooperative phenomena has shed light on fruitful theoretical and experimental problems with nonequilibrium dynamics of excited states.¹⁻⁸ It has been shown that many of these phenomena are concomitant with the change of crystal structure in which two important situations should be considered to understand their mechanism. In the first one, excitation of itinerant electrons induces the instability of the crystal lattice which leads to macroscopic structural change.⁹ The second one, which we focus on in this Rapid Communication, concerns the excitation of localized electrons in each molecular unit. In this case the structural change of the whole system follows the nucleation of molecular units in an excited state, and the spatial distribution of photoexcited electrons determines the dynamics of the nucleation process.¹⁰ Polydiacetylenes and spin-crossover complexes are typical examples of this case and the dynamical properties of these materials have been studied experimentally by ultrafast spectroscopy.^{3,4}

Among various experimental techniques, vibrational spectroscopy is a key to characterize photoinduced phases in these materials since the vibrational properties contain information on the nucleation dynamics complementary to the electronic properties. In spin-crossover complexes, for example, some of the phonon frequencies for the photoinduced phase are different from those for both the low-temperature phase and the high-temperature phase,¹¹ which shows that the structural properties are important to understand the nature of the photoinduced phase. On the other hand, we point out that the variation of phonon frequencies in transient regime should reflect the details of the dynamics of the nucleation processes, and that the time-resolved vibrational spectroscopy will be a powerful tool to understand the transient properties during the nucleation. In advance to such experiments with intense THz or X-ray light sources available in the near future, we aim at revealing the lattice dynamics of photoinduced nucleation processes focusing on its site-dependent properties theoretically, which corresponds to the transient lattice dynamics of photoinduced structural change.

Temporal behavior of physical properties is often characterized by various correlation functions such as two-point

correlation functions or power spectra. We note that they are efficient to analyze the dynamical properties of stochastic processes particularly when the relevant process is stationary. However, the nucleation dynamics in the photoinduced structural change necessarily involves the relaxation dynamics of excited states and thus is a non-stationary process, which shows that large fluctuation during the relaxation process plays a key role. We point out that the large deviation statistics is suitable for the analysis of the present problem, and we briefly introduce the method of analysis employed in this Rapid Communication referring to the results by Fujisaka and his co-workers.^{12,13} In the large deviation statistics a stochastic variable $x(t)$ is coarse-grained along the time axis as

$$\bar{x}_T(t) = \frac{1}{T} \int_t^{t+T} x(s) ds, \quad (1)$$

which converges to the long-time average of $x(t)$ for $T \rightarrow \infty$. The long-time behavior of the fluctuation of $x(t)$ is characterized by the fluctuation spectrum $S(u)$ defined by

$$S(u) = - \lim_{T \rightarrow \infty} \frac{1}{T} \log \langle \delta(\bar{x}_T(t) - u) \rangle, \quad (2)$$

where $\langle \dots \rangle$ denotes the average over t . Equation (2) shows that $S(u)$ is the inverse of a characteristic time scale of fluctuation of $x(t)$ in the long-time limit, and thus it describes the dynamics of the deviation from the long-time average of $x(t)$.

The relevant time scales of dynamical systems are often discussed by the autocorrelation function or its Fourier transform, the power spectra. In the large deviation statistics, the generalized power spectra $I_q(\Omega)$ are the correspondence to them. $I_q(\Omega)$ is a weighted average of the Fourier transform of the autocorrelation function defined by

$$I_q(\Omega) = \lim_{T \rightarrow \infty} \frac{1}{T} \frac{\langle | \int_0^T [x(t+s) - \bar{u}(q)] e^{-i\Omega s} ds |^2 e^{qT\bar{x}_T(t)} \rangle}{\langle e^{qT\bar{x}_T} \rangle}, \quad (3)$$

where $\bar{u}(q)$ satisfies the relation $dS/du(u=\bar{u}(q))=q$. q is called a selection parameter since Eq. (3) shows that $I_q(\Omega)$

for large value of q emphasizes the contribution of the dynamical properties for large value of $\bar{x}_T(t)$, and vice versa.

As for the model of materials, we employ a model of localized electrons coupled with an optical phonon mode which describes the essence of the photoinduced structural change. We consider an array of molecules on a square lattice with two electronic levels and a single phonon mode interacting with each other, which is described by the following Hamiltonian:

$$\mathcal{H} = \sum_{\vec{r}} \left\{ \frac{\hat{p}_{\vec{r}}^2}{2} + \frac{\omega^2 \hat{u}_{\vec{r}}^2}{2} + (\sqrt{2}\hbar\omega^3 s \hat{u}_{\vec{r}} + \varepsilon \hbar \omega + s^2 \hbar \omega) \hat{n}_{\vec{r}} + \lambda \sigma_x^{\vec{r}} \right\} + \sum_{\langle \vec{r}, \vec{r}' \rangle} [\alpha \omega^2 (\hat{u}_{\vec{r}} - \beta \hat{n}_{\vec{r}}) (\hat{u}_{\vec{r}'} - \beta \hat{n}_{\vec{r}'}) - \{V - W(\hat{u}_{\vec{r}} + \hat{u}_{\vec{r}'})\} \hat{n}_{\vec{r}} \hat{n}_{\vec{r}'}], \quad (4)$$

where $\hat{p}_{\vec{r}}$ and $\hat{u}_{\vec{r}}$ are the momentum and coordinate operators for the vibration mode of a molecule at site \vec{r} , respectively. Two electronic states are assigned to each site \vec{r} which are denoted by $|\downarrow\rangle_{\vec{r}}$ (ground state) and $|\uparrow\rangle_{\vec{r}}$ (excited state). $\sigma_i^{\vec{r}}$ ($i=x, y, z$) are the Pauli matrices which act only on the electronic states of the molecule at site \vec{r} . The nonadiabaticity in the dynamics is taken into account via “spin-flip” interaction between two electronic states as in typical organic molecules,¹⁴ as in typical organic molecules.¹⁴ $\hat{n}_{\vec{r}}$ denotes the density of the electron in $|\uparrow\rangle_{\vec{r}}$; i.e., $\hat{n}_{\vec{r}} = \sigma_z^{\vec{r}} + 1/2$. The second sum which gives the intermolecular interaction is taken over all the pairs on nearest neighbor sites, and we take into account the dipole-dipole interaction between excited units as well as the elastic interactions. We note that this Ising-like model is similar to the one to study the thermodynamical properties of the Jahn-Teller effect,¹⁵ while our aim is to reveal the nonequilibrium dynamics of the excited states of the model.

The molecules that we consider have two diabatic potential energy surfaces (PESs) which cross each other, and the nonadiabatic coupling $\lambda \sigma_x^{\vec{r}}$ acts to separate them into two adiabatic PESs. We chose the values of the parameters as: $\omega=1$, $\varepsilon=2.3$, $s=1.4$, $V=1.1$, $W=0.2$, $\alpha=0.1$, $\beta=2$, and $\lambda=0.2$, and the unit of time is taken to be $\tau=2\pi/\omega$. We note that the values of the parameters do not correspond to any specific material but the order of magnitude for the parameters is estimated referring to those for typical organic materials. As we have shown in Refs. 8 and 10, the numerical solution of the time-dependent Schrödinger equation for Hamiltonian (4) reveals the dynamics of the nucleation process triggered by converting some molecules to the Franck-Condon state. Details of the method of calculation are described in Ref. 16 and we do not mention it further to avoid redundancy. Here we only note that the nucleation process in the present model appears as the growth of “islands” of molecules in the excited electronic states $|\uparrow\rangle_{\vec{r}}$, and that it is driven by the propagation of coherent phonons.¹⁰

During the nucleation process, the electronic/vibrational states of individual molecules evolve with time giving influence on each other. For example, some molecules initially in the ground state convert to the excited electronic state and

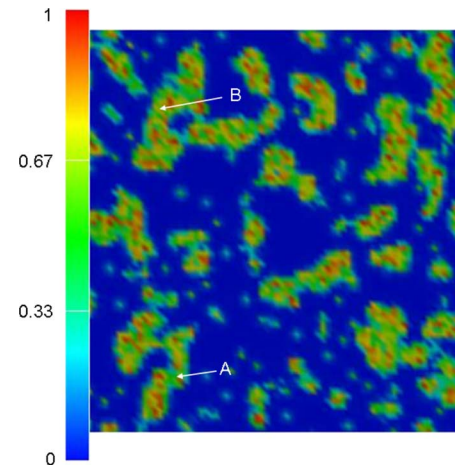


FIG. 1. (Color online) A palette map for $N(\vec{r}, t=5\tau)$ for a 80×80 system. 5% of the molecules is initially in the Franck-Condon state.

become a part of an “island.” Some molecules also go back to the ground state though it is in the Franck-Condon state initially. To exemplify the collective dynamics of photoinduced nucleation, we show in Fig. 1 a palette map for the excited-state population $N(\vec{r}, t) = \langle \Phi(t) | \hat{n}_{\vec{r}} | \Phi(t) \rangle$ for $t=5\tau$, where 5% of the molecules chosen at random are initially in the Franck-Condon state. The detail of the growth dynamics of the “islands” are discussed in Ref. 10.

In this Rapid Communication we study the dynamical properties of the deformation of the molecules $u(\vec{r}, t) = \langle \Phi(t) | \hat{u}_{\vec{r}} | \Phi(t) \rangle$ by regarding them as stochastic variables. The other sites are treated as a reservoir in this theoretical framework, and thus the microscopic detail of them is traced out by averaging over electronic/vibrational degrees of freedom. We selected two molecules at site A ($\vec{r}=\vec{r}_A$) and B ($\vec{r}=\vec{r}_B$) shown by the arrows in Fig. 1 and calculated $N(\vec{r}, t)$ and $u(\vec{r}, t)$ as a function of t . Figure 2 shows the calculated results of $N(\vec{r}, t)$ and $u(\vec{r}, t)$.

We first point out that both molecules A and B are initially in the ground state ($N(\vec{r}_A, 0) = N(\vec{r}_B, 0) = 0$), and that the overall behavior of $N(\vec{r}, t)$ and $u(\vec{r}, t)$ is similar, i.e., both proper-

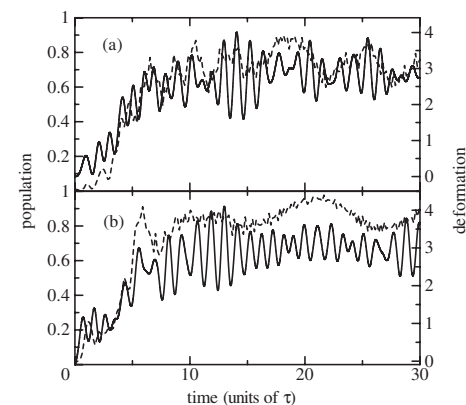


FIG. 2. The excited-state population $N(\vec{r}, t)$ (dashed lines) and the deformation $u(\vec{r}, t)$ (solid lines) for (a) molecule A ($\vec{r}=\vec{r}_A$) and (b) molecule B ($\vec{r}=\vec{r}_B$) shown by the arrows in Fig. 1.

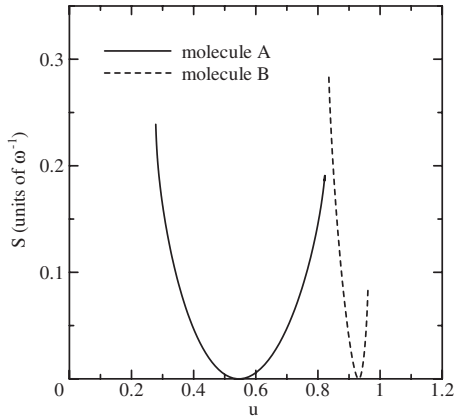


FIG. 3. The fluctuation spectrum $S(u)$ of the lattice deformation $u(\vec{r}, t)$ for molecules A and B.

ties increase or decrease according to the conversion between $|\uparrow\rangle_{\vec{r}}$ and $|\downarrow\rangle_{\vec{r}}$. Although we found that temporal oscillation is clearly seen only in $u(\vec{r}, t)$, we stress that there is no remarkable difference between the two properties for individual molecules.

When we apply the method of the large deviation analysis to $u(\vec{r}, t)$, qualitative difference between molecules A and B becomes apparent. We first calculated the fluctuation spectrum $S(u)$ for molecules A and B and the results are shown in Fig. 3. We found that the domain of u for $S(u)$ is quite different between the two molecules, i.e., $S(u)$ for molecule A is defined in a wider domain of u than that for molecule B. When multiple time-scales exist in the long-time dynamics of $u(\vec{r}, t)$, $S(u)$ is defined in a finite domain of u . In this case various temporal fluctuation with finite lifetime exists in the system [refer to Eq. (2)], which also reflects the influence of the other molecules. To be more precise, $S(u)$ shows the dynamics of the “islands” that molecule A or B belongs to through the intermolecular interactions, and thus we found that $S(u)$ reveals the detail of the nucleation dynamics at each site.

We note that the fluctuation spectra for molecule B is defined in a narrow domain of u , which is reminiscent of the motion of deterministic variables, i.e., $S(u)$ is composed of a single point on the u - S plane for deterministic variables. We conclude that the fluctuation of the motion of molecule B is small although $u(\vec{r}, t)$ is affected by the intermolecular interaction. Thus, we point out that the stochastic features of $u(\vec{r}, t)$ deviate site by site depending on the detail of the microscopic state of the system characterized by the time-evolution of the surrounding molecules and/or the adjacent “islands” of excited molecules.

The calculated results of $S(u)$ show that the dynamics of individual molecules is different from each other. We consider that this difference reflects on the relevant time scales for $u(\vec{r}, t)$, and thus calculated the generalized power spectra $I_q(\Omega)$. Figures 4(a) and 4(b) show contour plots of $I_q(\Omega)$ for molecules A and B. The selection parameter q enables us to separately discuss the dynamics of $u(\vec{r}, t)$ with regard to the magnitude of the deformation, which shows that $I_q(\Omega)$ contains information on the dynamics before/after electronic transition between $|\uparrow\rangle_{\vec{r}}$ and $|\downarrow\rangle_{\vec{r}}$. To be more precise, $I_q(\Omega)$

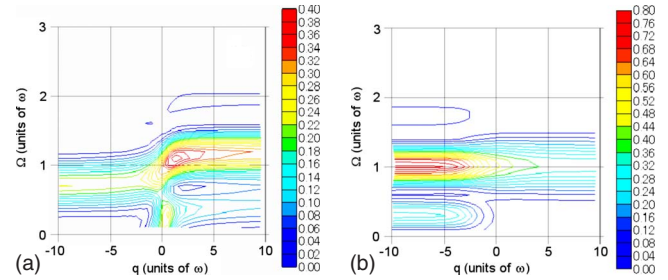


FIG. 4. (Color online) A contour plot of the generalized power spectra $I_q(\Omega)$ for $u(\vec{r}, t)$ for (a) molecule A and (b) molecule B. Ω and q are represented in units of ω .

for negative values of q embosses the dynamics before the conversion from $|\downarrow\rangle_{\vec{r}}$ to $|\uparrow\rangle_{\vec{r}}$, while that for positive q values reflects the dynamics after the conversion.

Figures 4(a) and 4(b) show that the characteristic frequency of the oscillation of $u(\vec{r}, t)$ is different for $q > 0$ and $q < 0$. In the case of molecule A, the main peak of $I_q(\Omega)$ for $q < 0$ is observed at $\Omega \sim 0.7\omega$ which corresponds to the phonon frequency with $|\vec{k}|=0$.⁸ Thus, molecule A vibrates synchronously with the surrounding molecules before the conversion takes place. After the conversion, however, this peak disappears and those at $\Omega \sim 1.1\omega$ and 2ω emerge in the generalized power spectra, which means that the phonons with larger value of $|\vec{k}|$ are relevant to the lattice motion of the molecule. To understand this peak shift, we point out that, after molecule A is absorbed into an “island” of excited molecules during the nucleation process, its motion is influenced by the coalescence of the “islands.” Since the lattice motion in different “islands” is not synchronized with each other, the coherence of the molecular vibration within an “island” is lost by the coalescence. As a result, the phase of $u(\vec{r}, t)$ for molecule A becomes different from that of the surrounding molecules and thus the motion of molecule A becomes fluctuating as shown in Fig. 3.

For molecule B, the behavior of $I_q(\Omega)$ is qualitatively different from that for molecule A. The main peak of $I_q(\Omega)$ lies at $\Omega \sim \omega$ irrespective of the value of q , which shows that the vibration of a single molecule or the corresponding phonon plays an important role in the dynamics of molecule B. Furthermore, for $q < 0$, additional peaks at $\Omega = 0.3\omega$ and 1.8ω are present and disappear as q increases. These features reflect the dynamics of molecule B in which the molecule is absorbed into a certain “island” during the early stage of relaxation, and the effect of coalescence of “islands” is not relevant afterwards. Thus, fluctuation of $u(\vec{r}, t)$ is small compared with that of molecule A as shown in Fig. 3.

The above results show that the characteristic phonon frequencies in the course of nucleation are different between the molecules. We stress that the present results show that the relevant phonon frequencies for the photoinduced phase differ from those for both the low-temperature phase or the high-temperature phase.¹¹ In particular, the initial nucleation processes involve local structure change, which appears as a change of vibrational dynamics in transient regime. Thus, by studying the distribution of the frequency shift, we will find the details of the nucleation dynamics in microscopic scale. In other words, by time-resolved vibrational spectroscopy,

we are able to discuss the transient properties of the nucleation processes, e.g., growth dynamics and/or coalescence of the nuclei, as well as the characterization of the photoinduced phase in macroscopic scale. It also helps us understand this aspect to consider that we have focused on the behavior of a single molecule in the large deviation analysis. In the present calculations the rest of the system is regarded as reservoir and the details of their influence are not explicitly taken into account. However, the present results show that the dynamics of the growth and/or coalescence of “islands” affects the vibrational properties of a single molecule even in this case, which means that they contain important information on the dynamics of the whole system.

Phonon frequency shift caused by photoinduced cooperativity has also been observed in itinerant electron systems.¹⁷ Since itinerancy of electrons induces long-range interaction between the deformation of molecules, effective interaction between “islands” is modulated by itinerant electrons/excitons. However, local structural change takes place in a similar manner to the present case qualitatively as far as nucleation is present in the early stage of relaxation process. Hence, the lattice dynamics has site-dependent features even in itinerant electron systems. In the case of organic salts,¹⁷ for example, we consider that the detail of the relaxation

dynamics will be revealed by precise measurement of relevant vibrational frequencies in coherent regime.

We mention a possibility of coherent control methods¹⁸ of the nucleation processes. Since the characteristic frequencies are different site by site in the nucleation, we point out that it is possible to control the growth of “islands” by irradiating laser pulses which are resonant to one of the characteristic modes of certain sites. To be more precise, site-selective excitation or deexcitation of molecules will be possible by appropriately designed laser pulses, which means that nanoscale control of photoinduced cooperativity will be possible by laser pulses beyond the diffraction limit. Typically THz laser pulses with narrow spectral width are suitable for this purpose, though the effect of irradiated laser pulses should be examined by further calculations.

One of the authors (K.I.) is grateful to K. Takaoka, H. Asai, and S. Nunoue for helpful advice. This work was supported by Grand challenges in next-generation integrated nanoscience, MEXT, Japan, and the numerical calculations were carried out on the computers at the Research Center for Computational Science, National Institutes of Natural Sciences.

*ishida@arl.rdc.toshiba.co.jp

¹ *Photoinduced Phase Transitions*, edited by K. Nasu (World Scientific, Singapore, 2004).

² K. Yonemitsu and K. Nasu, *Phys. Rep.* **465**, 1 (2008).

³ S. Koshihara, Y. Tokura, K. Takeda, and T. Koda, *Phys. Rev. Lett.* **68**, 1148 (1992); *Phys. Rev. B* **52**, 6265 (1995).

⁴ A. Mino, Y. Ogawa, S. Koshihara, C. Urano, and H. Takagi, *Mol. Cryst. Liq. Cryst.* **314**, 107 (1998).

⁵ N. O. Moussa, G. Molnár, S. Bonhommeau, A. Zwick, S. Mouri, K. Tanaka, J. A. Real, and A. Bousseksou, *Phys. Rev. Lett.* **94**, 107205 (2005).

⁶ K. Koshino and T. Ogawa, *Phys. Rev. B* **58**, 14804 (1998).

⁷ H. Mizouchi and K. Nasu, *J. Phys. Soc. Jpn.* **69**, 1543 (2000).

⁸ K. Ishida and K. Nasu, *Phys. Rev. B* **76**, 014302 (2007).

⁹ D. M. Fritz, D. A. Reis, B. Adams, R. A. Akre, J. Arthur, C. Blome, P. H. Bucksbaum, A. L. Cavalieri, S. Engemann, S. Fahy, R. W. Falcone, P. H. Fuoss, K. J. Gaffney, M. J. George, J. Hajdu, M. P. Hertlein, P. B. Hillyard, M. Horn-von Hoegen, M. Kammler, J. Kaspar, R. Kienberger, P. Krejčík, S. H. Lee, A. M.

Lindenberg, B. McFarland, D. Meyer, T. Montagne, E. D. Murray, A. J. Nelson, M. Nicoul, R. Pahl, J. Rudati, H. Schlarb, D. P. Siddons, K. Sokolowski-Tinten, Th. Tschentscher, D. von der Linde, and J. B. Hastings, *Science* **315**, 633 (2007).

¹⁰ K. Ishida and K. Nasu, *Phys. Rev. Lett.* **100**, 116403 (2008); *Phys. Rev. B* **77**, 214303 (2008).

¹¹ T. Tayagaki and K. Tanaka, *Phys. Rev. Lett.* **86**, 2886 (2001).

¹² H. Fujisaka and M. Inoue, *Prog. Theor. Phys.* **77**, 1334 (1987).

¹³ H. Fujisaka and M. Inoue, *Phys. Rev. A* **41**, 5302 (1990).

¹⁴ L. Salem, *Science* **191**, 822 (1976).

¹⁵ K. Boukheddaden, *Prog. Theor. Phys.* **112**, 205 (2004).

¹⁶ K. Ishida and K. Nasu, *Comput. Phys. Commun.* **180**, 1489 (2009).

¹⁷ S. Iwai, K. Yamamoto, A. Kashiwazaki, F. Hiramatsu, H. Nakaya, Y. Kawakami, K. Yakushi, H. Okamoto, H. Mori, and Y. Nishio, *Phys. Rev. Lett.* **98**, 097402 (2007).

¹⁸ S. A. Rice and M. Zhao. *Optical Control of Molecular Dynamics* (Wiley, New York, 2000).